Aristolochic acid suppresses DNA repair and triggers oxidative DNA damage in human kidney proximal tubular cells

YA-YIN CHEN[1,5], JING-GUNG CHUNG[2], HSIU-CHING WU[3], DA-TIAN BAU[1], KUEN-YUH WU[1,6],
SHUNG-TE KAO[1,5], CHIEN-YUN HSIANG[4*], TIN-YUN HO[1*] and SU-YIN CHIANG[1*]

[1]School of Chinese Medicine, [2]Department of Biological Science and Technology, [3]School of Post-Baccalaureate
Chinese Medicine, [4]Department of Microbiology, China Medical University, Taichung; [5]Department of Chinese Medicine,
China Medical University Hospital, Taichung; [6]Institute of Occupational Medicine and Industrial Hygiene,
College of Public Health, National Taiwan University, Taipei, Taiwan

Abstract. Aristolochic acid (AA), derived from plants of the *Aristolochia* genus, has been proven to be associated with aristolochic acid nephropathy (AAN) and urothelial cancer in AAN patients. In this study, we used toxicogenomic analysis to clarify the molecular mechanism of AA-induced cytotoxicity in normal human kidney proximal tubular (HK-2) cells, the target cells of AA. AA induced cytotoxic effects in a dose-dependent (10, 30, 90 μM for 24 h) and time-dependent manner (30 μM for 1, 3, 6, 12 and 24 h). The cells from those experiments were then used for microarray experiments in triplicate. Among the differentially expressed genes analyzed by Limma and Ingenuity Pathway Analysis software, we found that genes in DNA repair processes were the most significantly regulated by all AA treatments. Furthermore, response to DNA damage stimulus, apoptosis, and regulation of cell cycle, were also significantly regulated by AA treatment. Among the differentially expressed genes found in the dose-response and time-course studies that were involved in these biological processes, two up-regulated (*GADD45B, NAIP*), and six down-regulated genes (*TP53, PARP1, OGG1, ERCC1, ERCC2,* and *MGMT*) were confirmed by quantitative real-time reverse transcription polymerase chain reaction (qRT-PCR). AA exposure also caused a down-regulation of the gene expression of antioxidant enzymes, such as superoxide dismutase, glutathione reductase, and glutathione peroxidase. Moreover, AA treatment led to increased frequency of DNA strand breaks, 8-hydroxydeoxyguanosine-positive nuclei, and micronuclei in a dose-dependent manner in HK-2 cells, possibly as a result of the inhibition of DNA repair. These data suggest that oxidative stress plays a role in the cytotoxicity of AA. In addition, our results provide insight into the involvement of down-regulation of DNA repair gene expression as a possible mechanism for AA-induced genotoxicity.

Introduction

Aristolochic acid (AA), a mixture of structurally-related nitrophenanthrene carboxylic acids, was first detected in *Aristolochia clematitis* in 1943 (1). Aristolochic acid I (AAI) and Aristolochic acid II (AAII) are the two main active compounds of plants from the genus *Aristolochia*. Natural products containing AA were used in some pharmaceutical preparations as anti-inflammatory agents; moreover, many formulae containing *Aristolochia* plants are commonly used as traditional medicine in Eurasia, South America and West Africa (2-4). However, its use gradually declined after Mengs *et al* reported that it was carcinogenic in rats (5). Most countries now ban or severely restrict the use of plants of the genus *Aristolochia* based on a multitude of studies that have shown that AA is nephrotoxic in humans (6-10). Aristolochic acid nephropathy (AAN) is characterized by initially normal blood pressure, early severe anemia, mild tubular proteinuria, and rapid progression to renal failure within months up to 2 years (11). The pathology of AAN shows extensive hypo-cellular interstitial fibrosis associated with tubular atrophy and global glomerular sclerosis (12). Urothelial malignancy of upper urinary tract has been found in 40-46% of patients exposed to AA (13,14). Two population-based studies by Lai *et al* found that consumption of AA-containing Chinese herbal products was associated with an increased risk of end-stage renal disease and urinary tract cancer in a dose-dependent manner (15,16). This finding is similar to reports that show that high cumulative doses of AA can induce nephropathy in humans (17) and that cumulative doses >200 grams of ingested Aristolochia is a significant risk factor for urothelial carcinoma in Belgian AAN patients (13,14).

The carcinogenic effects of AA are considered to be associated with the formation of covalent AA-DNA adducts, which have been detected in affected kidneys of Belgian

---

Correspondence to: Dr Su-Yin Chiang, School of Chinese Medicine, China Medical University, No 91, Hsueh-Shih Road, Taichung 404, Taiwan
E-mail: sychiang@mail.cmu.edu.tw

*Contributed equally

patients with AAN (18,19) and in rodent tissues (20,21). Therefore, it is important to study the mechanism of metabolic activation of AA and the formation of AA-DNA adducts. AAI and AAII are metabolized to reactive intermediates that bind covalently to DNA *in vitro* and *in vivo* (18,20). Experiments on the enzymatic activation of AA by xanthine oxidase, DT-diaphorase, and cytosolic nitroreductase have confirmed that nitroreduction is crucial in the metabolic activation of AA (20). Other studies have shown that AA can be activated via nitroreduction by cytochrome P450 (CYP) 1A1, CYP1A2, and NADPH:CYP reductase (22-26). AA forms covalent DNA adducts and deoxyadenosine is the major target of modification. Broschard *et al* (27) found that dA-AAI, dG-AAI and dA-AAII severely block DNA replication. AA-adenine adducts have a higher mutagenic potential compared with the AA-guanine adducts and AT→TA transversion mutation has been found in *ras* gene of AA-exposed rodent tissues and in *P53* gene of tissues in AAN patients. Similarly, in AAN patients, one major (dA-AAI) and two minor (dG-AAI and dA-AAII) DNA adducts were detected in renal and urinary tissues (13,18,19,28-30).

AA-induced cytotoxicity and genotoxicity have been studied in several biological systems over the past years. Balachandran *et al* (31) and Li *et al* (32) have used a porcine proximal tubular epithelial cell line (LLC-PK1) to study DNA damage, cell cycle perturbations, and cell apoptosis induced by AA. Human urinary tract epithelium cells (SV-HUC-1), human hepatoma HepG2 cells, and human colo-rectal cancer cells (HCT 116) (33-35) have also been used to study the cytotoxicity or genotoxicity of AA. Chen *et al* (36) have shown that more cancer-related genes were significantly altered in target (kidney) tissues than in non-target (liver) tissues in AA-treated rats, suggesting that studies on the toxic effects of AA should be conducted in renal cells.

In this study, we used toxicogenomic analysis to investigate the toxic effects of AA in normal human proximal tubular (HK-2) cells, the target cells of AA. We then tried to elucidate the molecular mechanism of AA-induced toxicity by applying microarray analysis to explore the changes in gene expression patterns in cells exposed to AA. Our results indicate that the decreased expression of DNA repair genes may contribute to the observed increase in 8-OHdG and micronuclei formation in HK-2 cells and may partly explain the genotoxic effects of AA.

Materials and methods

Cell culture. The human kidney-2 (HK-2), an immortalized cell line of renal proximal tubular epithelial cells from normal adult human kidney, were obtained from Bioresource Collection and Research Center (Hsinchu, Taiwan; BCRC 60097). HK-2 cells were grown in keratinocyte serum-free basal medium (Gibco) supplemented with recombinant epidermal growth factor (5 ng/ml) and bovine pituitary extract (50 μg/ml) without antibiotics at 37°C in a 5% CO_2 incubator.

Drug treatment. Aristolochic acid sodium salt, a mixture of AA I (41%) and AA II (56%) (Sigma) was dissolved in double-distilled water and stored at -30°C. HK-2 cells were seeded in 75T flasks or 25T flasks and incubated for over-night before AA treatment. Various concentrations of AA (10, 30, 90 μM) were exposed to HK-2 cells for 24 h or 30 μM AA was exposed for 1, 3, 6, 12 and 24 h. The control cells were placed in equal amounts of water.

3-[4,5-dimethylthiazol-2yl]-2,5-diphenyltetrazolium bromide (MTT) assay. After AA treatment for varied length of time, MTT was added to 75T flasks or 25T flasks to reach the final concentration of 0.5 mg/ml. After a 4-h incubation at 37°C in the dark, equal volume of 10% SDS (pH 2.0) was added to dissolve the MTT formazan. When the MTT formazan was dissolved completely, the samples in flasks were transferred to 96-well plates at a volume of 200 μl per well. The absorbance was measured at a test wavelength of 570 nm and a reference wavelength of 630 nm using a microplate reader. The relative survival of cell growth was calculated by the equation that follows: survival rate (%) = (Absorbance of AA-treated cells - absorbance of medium only/Absorbance of untreated cells - absorbance of medium only) x 100%.

RNA isolation and toxicogenomic analysis. Total RNAs were extracted from HK-2 cells collected from the dose and time-course study using RNeasy Mini kit (Qiagen, Valencia, CA). Total RNA was quantified using the Beckman DU800 spectro-photometer (Beckman Coulter, Fullerton, CA). Samples with A_{260}/A_{280} ratios >1.8 were further evaluated using Aglient 2100 Bioanalyzer (Agilent Technologies, Santa Clara, CA). The RNA samples with an RNA integrity number >8.0 were subjected to microarray analysis.

Microarray analysis was performed in triplicate as described previously (37). Briefly, fluorescence-labeled RNA targets were prepared from 5 μg of total RNA samples using MessageAmp™ aRNA kit (Ambion, Austin, TX) and Cy5 dye (Amersham Pharmacia, Piscataway, NJ). Triplicate fluorescent targets were hybridized overnight to the Human Whole Genome OneArray™ (Phalanx Biotech Group, Hsinchu, Taiwan), and non-specific targets were washed by three different washing steps, and the slides were dried by centrifugation and immediately scanned by an Axon 4000 scanner (Molecular Devices, Sunnyvale, CA). The Cy5 fluo-rescent intensity of each spot was analyzed by genepix 4.1 software (Molecular Devices). The signal intensity of each spot was corrected by subtracting background signals in the surrounding area. We filtered out control probes and background-corrected signal intensity of each spot. Spots were then normalized by the Limma package of the R program (38). Normalized data were tested for differential expression using the Gene Expression Pattern Analysis Suite v3.1 (39). We used the 'geneSetTest' function in the Limma package to test which biological pathways were affected by AA in HK-2 cells. This function computes a p-value to test the hypothesis that the selected genes in a pathway tend to be differentially expressed. We have submitted the original microarray data to Gene Expression Omnibus (GEO), series number GSE18243. Two samples (mock, treatment) and one series (mock + treatment) are included. The sample numbers are GSM455880 (treatment) and GSM455881 (mock).

Table I. Primer sequences of selected genes for qRT-PCR.

Gene	Primer sequence
ERCC1	Sense: 5'-TCTCCCGGGTGACTGAATGT-3' Antisense: 5'-GCGATGAGCTGTTCCAGAGAT-3'
ERCC2	Sense: 5'-GGCAAAGTGTCCGAGGGAAT-3' Antisense: 5'-CCTTGAGAATGCGGCTCTGT-3'
GADD45B	Sense: 5'-TGTACGAGTCGGCCAAGTTG-3' Antisense: 5'-ATTTGCAGGGCGATGTCATC-3'
MGMT	Sense: 5'-CCTGGCTGAATGCCTATTTCC-3' Antisense: 5'-TGTCTGGTGAACGACTCTTGCT-3'
NAIP	Sense: 5'-CTGGATGCTGTCCCCTGTTAA-3' Antisense: 5'-AGGAGCTGGTCACAGATGATACTG-3'
OGG1	Sense: 5'-TTCCAAGAGGTGGCTCAGAAAT-3' Antisense: 5'-CGATGTTGTTGTTGGAGGAACA-3'
PARP	Sense: 5'-GGAGTCGGCGATCTTGGA-3' Antisense: 5'-AGTAATAGGCATCGCTCTTGAAGAC-3'
TP53	Sense: 5'-GGGTTAGTTTACAATCAGCCACATT-3' Antisense: 5'-GGGCCTTGAAGTTAGAGAAAATTCA-3'

Quantitative real-time reverse transcription polymerase chain reaction (qRT-PCR). The expression levels of DNA repair-related genes were further validated by qRT-PCR. Total RNA was used as a template for reverse transcription using the RNA Reverse Transcription Kit from ABI (Applied Biosystems). Quantitative PCR was performed using 1 μl of cDNA, 2X SYBR-Green PCR Master Mix (Applied Biosystems, Foster City, CA, USA). The reaction conditions were as follows: 10 min at 95˚C followed by 40 cycles of 15 sec at 95˚C, 1 min at 60˚C. Each assay was run on an Applied Biosystems 7300 real-time PCR system in triplicates. Relative amount of mRNA was calculated using the comparative C_T method. The primer sets for selected genes are shown in Table I.

Alkaline single-cell gel electrophoresis (comet assay). HK-2 cells were treated with 10, 30, 90, 150 μM of AA for 3 or 24 h, and 100 μM of H_2O_2 (positive control) for 30 min. After treatment with AA, cells were harvested for the examination of DNA damage by using the Comet assay. Seventy microliters of 0.5% of normal melting point agarose (NMP) and 0.5% low melting point agarose (LMP) in PBS (pH 7.4) were covered on the slides, and allowed to dry. Ten microliters of cell suspension (1x10^4 cells) were gently mixed with 70 μl of 0.5% of LMP in PBS (pH 7.4), and take 70 μl of this suspension rapidly layered onto the slides precoated with the mixtures of 0.5% of NMP and 0.5% of LMP, and covered with a coverslip. Then the coverslip was removed and the cells embedded in agarose were immersed in a freshly made lysis solution (2.5 M NaCl, 100 mM Na$_2$EDTA, 10 mM Tris and 1% Triton X-100 at pH 10.0) for 1 h at 4˚C. The slides then were placed on a horizontal gel electrophoresis tank and the DNA was allowed to unwind for 20 min in freshly prepared alkaline electrophoresis buffer containing 0.3 M of NaOH and 1 mM of Na$_2$EDTA (pH >13). Thereafter, electrophoresis (25 V, 300 mA) was conducted for 30 min at 4˚C. After electrophoresis, the slides were then soaked in a cold neutralizing buffer (0.4 M Tris buffer, pH 7.5) to neutralize the excess alkali at 4˚C for 15 min. Slides were dried in methanol for 5 min, and stained with propidium iodide (5 μg/ml). Comet length was analyzed using CometScore software.

Immunostaining for 8-OHdG. HK-2 cells were seeded on coverslips and treated with AA (10, 30 or 90 μM) for 24 h. The coverslips were fixed with cold acetone for 10 min at -20˚C, air-dried at room temperature, and stored at -20˚C if not processed immediately. Before staining, the cells were rehydrated in PBS and treated with RNase (100 μg/ml) in Tris buffer (pH 7.5; 10 mM Tris-HCl, 0.4 M NaCl) at 37˚C for 50 min and proteinase K (1 μg/ml) for 7 min at room temperature. Samples were denatured in 4 N HCl for 5 min and neutralized with 50 mM Tris-base for 4 min. In order to block endogenous peroxidase, samples were incubated with 3% H_2O_2 in methanol for 15 min. Immunocytochemistry was performed using a Novolink Polymer Detection System (Novocastra). Briefly, non-specific binding was blocked by protein block (RE7166, 0.4% Casein in phosphate-buffered saline) for 30 min at room temperature and incubated with anti-8-hydroxydeoxyguanosine (8-OHdG) monoclonal antibody N45.1 (Fukuroi, Japan, 1:200 dilution) overnight at 4˚C. After rinsing with PBS, post primary block (RE7167, 10% animal serum) was incubated for 30 min, followed by Novo-Link™ polymer (RE7168, anti-mouse/rabbit IgG-Poly-HRP)
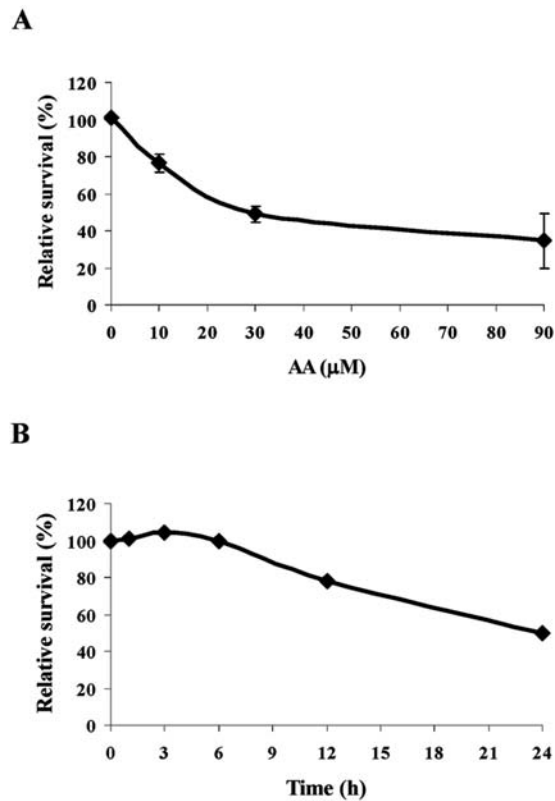
A

B

Figure 1. The cytotoxicity of various doses and time intervals of AA in HK-2 cells. HK-2 cells in 75T flasks or 25T flasks were treated with 10, 30 and 90 μM of AA (A) and 30 μM of AA for 1, 3, 6, 12 and 24 h (B). The cell viability was measured by MTT assay. Values are mean ± standard deviation of three independent experiments. ***P<0.001, indicate significant difference as compared to control group.

for 30 min. Slides were treated with diaminobenzidine to localize peroxidase and mounted on a cover glass. 8-OHdG-stained cells were then detected under light microscopy.

Western blot analysis. HK-2 cells treated with or without AA were harvested, lysed in lysis buffer, and centrifuged at

10,000 x g for 5 min. The supernatant was collected and protein concentrations were determined using the Bradford colorimetric assay. After denaturing by heating at 95°C for 5 min, 45 μg of each protein lysate were loaded in each lane in sample buffer, separated on 10% SDS-PAGE. The separated proteins were transferred onto nitrocellulose membranes and blocked with 5% non-fat milk for 1 h at room temperature. The membranes were incubated overnight at 4°C with the rabbit anti-OGG1 antibody (Novus Biologicals, Littleton, CO), mouse anti-p21 antibody, rabbit anti-c-fos antibody, mouse anti-caspase-3 antibody, mouse anti-Bax antibody and mouse anti-α-tubulin antibody (Santa Cruz Biotechnology) at 1:1000 dilution. After washing 10 min with TBS-Tween three times, the membranes were incubated with a 1:10000 dilution of goat anti-rabbit horseradish peroxidase (HRP)-conjugated antibody (Santa Cruz Biotechnology) for 1 h at room temperature. Finally, the blots were visualized by ECL.

Micronucleus test. HK-2 cells were seeded on coverslips and treated with AA (10 or 30 μM). After 24-h incubation, cytochalasin B was added to a final concentration of 3 μg/ml for 16-24 h to obtain binucleated cells. The cells were fixed with methanol at 4°C for 30 min and air-dried for 10 min. For staining, the slides were incubated with acridine orange (0.1 mg/ml) in the dark for 10 min, wash twice with buffer, and mounted for microscopy. The analysis was performed under fluorescent microscope with 488 nm excitation wavelength. Small round or ovoid-shaped intracytoplasmic bodies with a diameter of 1/3-1/20 of the main nucleus in binucleated cells were scored as micronuclei. A total of 1000 binucleated cells from 2 slides were scored for each treatment. The averages of three independent experiments are shown.

Statistical analysis. Data are presented as mean ± SD. Student's t-test was used for comparisons between the control and AA-treated groups. A value of p<0.05 was considered to be statistically significant.

Table II. Biological processes significantly regulated by AA in HK-2 cells.

Biological processes	Genes	P-values		
		10 μM AA	30 μM AA	90 μM AA
DNA repair	166	3.15×10^{-7}	7.70×10^{-5}	1.75×10^{-7}
Response to DNA damage stimulus	122	5.40×10^{-7}	2.00×10^{-4}	2.20×10^{-6}
Mitochondrial transport	28	1.00×10^{-4}	3.50×10^{-3}	1.99×10^{-2}
Lipid metabolic process	195	3.00×10^{-4}	2.00×10^{-1}	1.90×10^{-3}
Apoptosis	295	4.00×10^{-4}	1.60×10^{-3}	1.19×10^{-5}
Extracellular matrix organization and biogenesis	17	1.80×10^{-3}	9.43×10^{-6}	8.21×10^{-2}
DNA-dependent DNA replication	42	2.10×10^{-3}	1.00×10^{-3}	2.29×10^{-2}
Extracellular structure organization and biogenesis	13	4.30×10^{-3}	1.31×10^{-2}	3.40×10^{-1}
Regulation of cell cycle	181	1.27×10^{-2}	2.33×10^{-2}	8.71×10^{-6}
Negative regulation of cell proliferation	116	1.09×10^{-2}	1.93×10^{-1}	2.33×10^{-2}

The biological pathways affected by AA in HK-2 cells were examined by GeneSetTest' function in the Limma package. This function computes a p-value to test the hypothesis that the selected genes in a pathway tend to be differentially expressed (n=3).
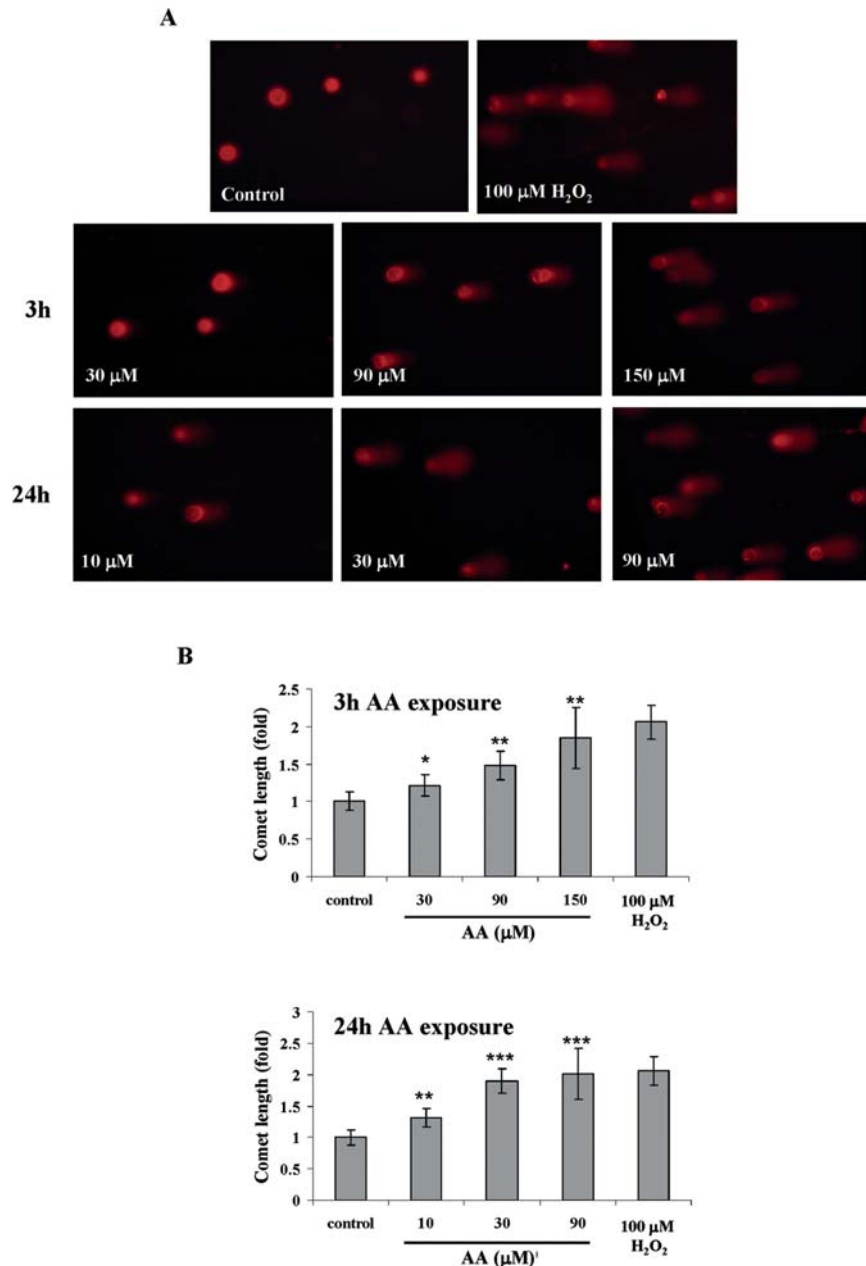
Figure 2. Induction of DNA strand breaks in HK-2 cells. AA induced DNA damage in HK-2 cells was examined by Comet assay and DNA gel electrophoresis. The HK-2 cells were incubated with various concentrations of AA for 3 or 24 h and DNA damage was determined by Comet assay. The cell pellet was resuspended in LMP agarose for comet analysis and cells embedded in agarose were lysed. Thereafter, DNA was allowed to unwind under alkaline buffer and electrophoresis was conducted under 25 V for 30 min. Finally, slides were neutralized, dried, and then stained with propidium iodide (5 μg/ml). (A) Representative photomicrographs from three independent experiments (original magnification, x200). (B) The quantification of comet length. *P<0.05, **P<0.01, ***P<0.001.

Results

Cytotoxicity. We examined cell viability in 25T flasks or 75T flasks by MTT assay after exposing HK-2 cells to various concentrations of AA (10, 30 or 90 μM) for 24 h or to 30 μM AA for 1, 3, 6, 12 and 24 h. There is little or no effect on cell survival at low dose of AA (10 μM) or in short exposure time to 30 μM AA (up to 12 h). A 24-h exposure to 10, 30, and 90 μM of AA resulted in a dose-dependent decrease in kidney cell growth with an IC$_{50}$ value of 30 μM. The relative survival rate of cells treated with 10 μM AA was 76.5±5.0, that of cells exposed to 30 μM AA was 49.0±4.2, and that of cells treated with 90 μM AA was 34.6±14.7 (Fig. 1A). The

relative survival of cells treated with 30 μM AA for 1, 3, 6, 12 and 24 h was: 101.1±0.9, 104.0±0.8, 99.8±1.0, 77.9±0.4 and 50.0±0.2 (Fig. 1B).

Gene expression profiles. We used unsupervised analysis to predict significant differences in gene expression in HK-2 cells in response to 10, 30 and 90 μM of AA treatment. As shown in Table II, genes in the DNA repair pathway were the most significantly regulated. Selected differentially expressed genes related to stress response, cell cycle, apoptosis, fibrogenic response, and biotransformation were listed in Table III. The selected DNA repair genes significantly regulated by AA in HK2 cells included genes in pathways of

Table III. Selected stress response-, cell cycle-, apoptosis-, fibrogenic response- and biotransformation-related genes significantly regulated by AA in HK-2 cells.

Gene symbol	Annotation	Fold change ± SD		
		10 μM AA	30 μM AA	90 μM AA
Stress response				
DDIT3	DNA-damage-inducible transcript 3	-	1.66±0.16[a]	4.03±0.12[b]
GADD45B	Growth arrest and DNA-damage-inducible, ß	2.68±0.16[a]	3.66±0.19[a]	3.00±0.15[a]
GADD45G	Growth arrest and DNA-damage-inducible, γ	-	5.08±0.33[a]	13.36±0.32[b]
GPX3	Glutathione peroxidase 3 (plasma)	-1.87±0.19[a]	-1.76±0.16[b]	-
GPX6	Glutathione peroxidase 6 (olfactory)	-	-2.56±0.22[a]	-2.10±0.17[a]
GSR	Glutathione reductase	-	-2.61±0.12[b]	-2.42±0.20[a]
HSPA14	Heat shock 70 kDa protein 14	1.89±0.07[c]	1.85±0.10[b]	1.41±0.06[b]
HSPC047	HSPC047 protein	1.97±0.25[a]	4.19±0.25[b]	4.60±0.27[b]
HSPC065	HSPC065 protein	1.87±0.29[a]	1.91±0.29[a]	-
MT1X	Metallothionein 1X	-1.83±0.23[a]	-1.45±0.12[a]	-
SOD3	Superoxide dismutase 3, extracellular	-1.51±0.16[a]	-2.09±0.11[b]	-
Cell cycle				
CCND2	Cyclin D2	-2.25±0.06[c]	-2.89±0.05[c]	-5.69±0.15[b]
CCNE1	Cyclin E1	-1.25±0.25[a]	-1.50±0.20[a]	-1.84±0.15[b]
CDKL1	Cyclin-dependent kinase-like 1 (CDC2-related kinase)	-1.68±0.21[a]	-1.79±0.24[a]	-
CDKN1A	Cyclin-dependent kinase inhibitor 1A (p21)	-1.64±0.17[a]	-	-
CDKN1B	Cyclin-dependent kinase inhibitor 1B (p27, Kip1)	-1.42±0.08[b]	-	-2.82±0.11[c]
CDKN2B	Cyclin-dependent kinase inhibitor 2B (p15, inhibits CDK4)	-1.54±0.12[b]	-1.33±0.11[a]	-1.58±0.12[b]
CDKN3	Cyclin-dependent kinase inhibitor 3 (CDK2-associated dual specificity phosphatase)	-1.91±0.25[a]	-2.49±0.09[c]	-
E2F3	E2F transcription factor 3	-1.21±0.07[a]	-1.51±0.12[a]	-1.84±0.06[c]
MDM2	Mdm2, p53 binding protein (mouse)	-1.41±0.11[a]	-1.57±0.08[b]	-
RB1	Retinoblastoma 1 (including osteosarcoma)	-	-1.44±0.18[a]	-2.24±0.20[b]
RBL2	Retinoblastoma-like 2 (p130)	-	-2.25±0.18[b]	-1.49±0.13[a]
TP53	Tumor protein p53 (Li-Fraumeni syndrome)	-1.90±0.14[a]	-1.50±0.08[a]	-1.34±0.05[b]
WEE1	WEE1 homolog (*S. pombe*)	-2.00±0.18[b]	-2.01±0.23[a]	-2.58±0.24[b]
Apoptosis				
BAX	BCL2-associated X protein	-	-	1.28±0.07[a]
BCL2L2	BCL2-like 2	-	-2.26±0.10[b]	-1.95±0.06[b]
BNIP3	BCL2/adenovirus E1B 19 kDa interacting protein 3	-2.04±0.19[b]	-2.76±0.20[b]	-3.60±0.17[b]
CASP3	Caspase-3, apoptosis-related cysteine protease	1.05±0.15[a]	1.40±0.17[a]	1.34±0.13[a]
CCL2	Chemokine (C-C motif) ligand 2	-	-1.86±0.19[a]	-3.54±0.31[b]
NAIP	Apoptosis inhibitor protein	3.25±0.38[a]	4.91±0.35[b]	3.25±0.10[c]
PRKCA	Protein kinase C, α	-	-1.41±0.09[b]	-2.92±0.17[b]
TNFRSF1B	Tumor necrosis factor receptor superfamily, member 1B	1.67±0.21[a]	1.61±0.25[a]	2.35±0.37[a]
TNFRSF21	Tumor necrosis factor receptor superfamily, member 21	1.46±0.09[a]	1.33±0.13[a]	1.88±0.12[b]
TNFSF6	Tumor necrosis factor (ligand) superfamily, member 6	-	3.46±0.25[a]	4.55±0.32[b]
Fibrogenic response				
FOS	v-fos FBJ murine osteosarcoma viral oncogene homolog	-	1.37±0.17[a]	1.97±0.20[b]
ITGB7	Integrin, ß 7	5.01±0.40[a]	12.22±0.12[c]	15.36±0.19[c]
LTBP2	Latent transforming growth factor ß binding protein 2	1.51±0.17[a]	2.47±0.20[b]	2.50±0.16[b]
MMP2	Matrix metalloproteinase 2	-1.75±0.31[a]	-2.10±0.22[a]	-1.64±0.21[a]
NBL1	Neuroblastoma, suppression of tumorigenicity 1	-1.12±0.12[a]	-1.37±0.16[a]	-1.27±0.11[a]
PLAU	Plasminogen activator, urokinase	1.32±0.10[a]	1.54±0.08[b]	-
SMAD4	SMAD, mothers against DPP homolog 4 (*Drosophila*)	-	1.77±0.14[a]	1.55±0.07[b]
STAT1	Signal transducer and activator of transcription 1, 91 kDa	-2.28±0.11[b]	-3.33±0.19[b]	-4.21±0.10[b]
TBRG4	Transforming growth factor ß regulator 4	1.71±0.13[b]	2.64±0.08[c]	4.17±0.21[b]

Table III. Continued.

Gene symbol	Annotation	Fold change ± SD		
		10 μM AA	30 μM AA	90 μM AA
Biotransformation				
CYP1A1	Cytochrome P450, family 1, subfamily A, polypeptide 1	3.22±0.24[a]	4.91±0.29[b]	4.85±0.25[b]
EPHX1	Epoxide hydrolase 1, microsomal (xenobiotic)	-	1.33±0.06[a]	1.11±0.01[c]
GNMT	Glycine N-methyltransferase	4.49±0.19[b]	7.94±0.13[b]	7.04±0.09[c]
GSTA2	Glutathione S-transferase A2	-	-1.85±0.09[b]	-2.18±0.26[a]
GTDC1	Glycosyltransferase-like 1	-2.00±0.14[b]	-2.60±0.14[b]	-4.34±0.22[b]
MGST2	Microsomal glutathione S-transferase 2	-	-1.95±0.19[a]	-2.09±0.18[a]
MGST3	Microsomal glutathione S-transferase 3	-1.49±0.11[b]	-2.15±0.14[a]	-1.90±0.13[a]
POR	P450 (cytochrome) oxidoreductase	-	1.46±0.08[b]	2.53±0.12[c]
XDH	Xanthine dehydrogenase	-	-2.28±0.31[a]	-2.05±0.36[a]

SD, standard deviation. [a]$P<0.05$, [b]$P<0.01$, [c]$P<0.001$ as compared to control cells, n=3.

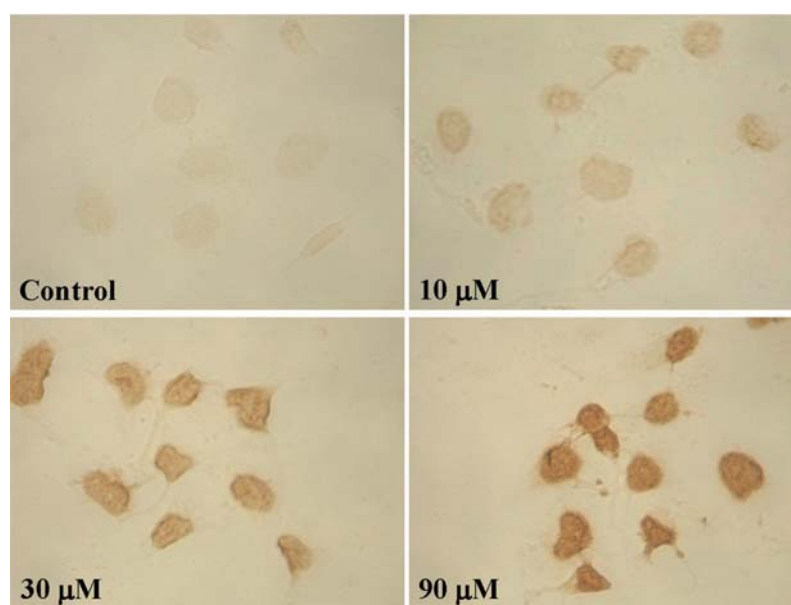

Figure 3. Induction of 8-OHdG by AA in HK-2 cells. HK-2 cells were treated with 10, 30, 90 μM of AA for 24 h. Then, the cells were immunostained for 8-OHdG using the N45.1 monoclonal antibody (1:200). Nuclei of HK-2 cells presented strong positive staining for 8-OHdG after AA exposure. Representative photomicrographs from three independent experiments are shown (original magnification, x400).

base excision repair, nucleotide excision repair, direct reverse repair, and mismatch repair (Table IV).

Tables V and VI show the comparison of expression of selected DNA repair genes and stress response genes from the dose and time-course response study by microarray and qRT-PCR in AA-treated HK-2 cells. A total of eight genes, including five DNA repair genes (ERCC1, ERCC2, MGMT, OGG1, and PARP1), two apoptosis-related genes (TP53 and NAIP), and stress one response-related gene (GADD45B) were chosen for verification by qRT-PCR. The expression levels of DNA repair-related genes in qRT-PCR correlated with the general trend of expression in the microarray analysis. Among genes involved in DNA repair pathway and stress response, the down-regulation of ERCC1, ERCC2, MGMT, OGG1 and TP53 by AA observed in the microarray analysis

was confirmed by qRT-PCR, with the most prominent effects at 24 h after AA exposure (Table VI).

Comet assay. AA induced DNA damage in HK-2 cells was examined by Comet assay. The results from Comet assay are presented in Fig. 2. Higher concentrations of AA led to longer DNA migration smears (Comet tail) (Fig. 2), and indicated that more DNA was damaged in the cells. These results showed that AA induced DNA damaged in HK-2 cells in a dose-dependent manner.

Immunostaining assessment of 8-OHdG. We evaluated the extent of oxidative damage of DNA using immunocyto-chemical staining of 8-OHdG, the most widely measured oxidative DNA damage. Fig. 3 shows representative

Table IV. Selected DNA repair genes significantly regulated by AA in HK-2 cells.

Gene symbol	Annotation	Fold change ± SD		
		10 μM AA	30 μM AA	90 μM AA
Base excision repair				
APEX2	APEX nuclease (apurinic/apyrimidinic endonuclease) 2	-1.52±0.16[a]	-1.51±0.19[a]	-2.06±0.15[b]
LIG3	Ligase III, DNA, ATP-dependent	-1.80±0.16[a]	-1.60±0.09[b]	-1.13±0.10
MPG	N-methylpurine-DNA glycosylase	-1.89±0.13[b]	-2.28±0.11[b]	1.02±0.15
OGG1	8-oxoguanine DNA glycosylase	-1.81±0.36	-2.53±0.23[a]	-2.12±0.42
PARP1	Poly (ADP-ribose) polymerase family, member 1	-1.32±0.17	-1.68±0.17[a]	-2.21±0.15[b]
SMUG1	Single-strand selective monofunctional uracil DNA glycosylase	-1.18±0.22	-1.51±0.11[a]	-1.64±0.16[a]
Nucleotide excision repair				
ERCC1	Excision repair cross-complementing rodent repair deficiency, complementation group 1	-2.53±0.22[b]	-2.76±0.20[b]	1.16±0.16
ERCC2	Excision repair cross-complementing rodent repair deficiency, complementation group 2	4.32±0.12[c]	-3.79±0.11[c]	-1.48±0.08[b]
PNKP	Polynucleotide kinase 3'-phosphatase	-4.18±0.24[b]	-3.51±0.18[b]	-1.26±0.10
RAD23A	RAD23 homolog A (*S. cerevisiae*)	-1.88±0.15[b]	-1.48±0.17[a]	-1.21±0.15
RAD23B	RAD23 homolog B (*S. cerevisiae*)	-1.38±0.16[a]	-1.53±0.16[a]	-2.33±0.21[a]
Direct reverse repair				
MGMT	O-6-methylguanine-DNA methyltransferase	-1.32±0.29	-2.60±0.31[a]	-1.56±0.32
Mismatch Repair				
POLD4	Polymerase (DNA-directed), δ 4	-1.56±0.12[b]	-1.78±0.13[b]	1.21±0.14
Homologous recombination				
NBS1	Nijmegen breakage syndrome 1 (nibrin)	-1.49±0.34	-1.86±0.24[a]	-4.32±0.26[b]
RAD18	RAD18 homolog (*S. cerevisiae*)	-1.86±0.20[a]	-1.61±0.13[b]	-1.39±0.11[a]
RAD54L	RAD54-like (*S. cerevisiae*)	-1.38±0.09[a]	-1.35±0.12[a]	1.42±0.13[a]
Non-homologous end joining				
BTG2	BTG family, member 2	-2.65±0.26[b]	-2.29±0.25[a]	-1.54±0.22[a]
CIB1	Calcium and integrin binding 1 (calmyrin)	-1.61±0.12[b]	-1.83±0.12[b]	1.64±0.09[b]
RFC3	Replication factor C (activator 1) 3, 38 kDa	-1.27±0.46	-1.54±0.12[a]	-2.18±0.16[b]
RFC4	Replication factor C (activator 1) 4, 37 kDa	-1.36±0.19	-1.61±0.21[a]	-1.69±0.21[a]

SD, standard deviation. [a]$P<0.05$, [b]$P<0.01$, [c]$P<0.001$ as compared to control cells, n=3.

immunostaining of 8-OHdG in HK-2 cells treated with or without AA. 8-OHdG was localized mainly in the nucleus of both control and AA-treated cells, and the staining intensity of 8-OHdG was greater in AA-treated group especially at the concentration of 90 μM than in the control group.

Western blot analysis. Protein levels of c-fos, OGG1, caspase-3, Bax, and p21 were analyzed by Western blot analysis in cells exposed to various concentration of AA (0, 10, 30 and 90 μM) for 24 h (Fig. 4). As expected, AA caused a significant dose-dependent increase in the expression of c-fos,

caspase-3, and Bax proteins in comparison to controls, and a decrease in the expression of OGG1 and p21 proteins.

Micronucleus test. The genotoxicity of AA was examined by the micronucleus test as a marker of chromosome alteration. Treatment with AA for 24 h induced a dose-dependent increase in the frequency of micronuclei formation in binucleated HK-2 cells. The frequency of micronuclei in control was 3.5±0.4, that of cells exposed to 10 μM AA was 10.2±1.4, and that of cells treated with 30 μM AA was 13.9±1.9 (Fig. 5).

Table V. Expression of selected DNA repair genes and stress response genes from dose response study by microarray and qRT-PCR in AA-treated HK-2 cells.

Gene	Microarray (Fold change ± SD)			qRT-PCR (Fold change)		
	10 μM AA	30 μM AA	90 μM AA	10 μM AA	30 μM AA	90 μM AA
ERCC1	-2.53±0.22[a]	-2.76±0.20[b]	-1.34±0.05[b]	-1.35	-1.27	-1.16
ERCC2	-4.32±0.12[c]	-3.79±0.11[c]	-1.48±0.08[b]	-1.75	-1.39	-1.69
GADD45B	2.68±0.16[b]	3.66±0.19[b]	2.99±0.15[b]	2.00	2.31	1.87
MGMT	-1.32±0.29	-2.60±0.31[a]	-1.56±0.32	-1.56	-2.63	-2.56
NAIP	3.25±0.38[a]	4.91±0.35[b]	3.25±0.10[c]	1.94	1.48	1.46
OGG1	-1.81±0.36	-2.53±0.23[b]	-2.12±0.42	-1.49	-1.56	-1.56
PARP1	-1.32±0.17	-1.68±0.17[a]	-2.21±0.15[b]	1.13	-1.14	-1.54
TP53	-1.90±0.14[a]	-1.50±0.08[a]	-1.34±0.05[b]	-1.82	-1.15	1.03

SD, standard deviation. [a]P<0.05, [b]P<0.01, [c]P<0.001 as compared to control cells, n=3 for microarray and qRT-PCR analysis.

Table VI. Expression of selected DNA repair genes from time-course study by microarray and qRT-PCR in AA-treated HK-2 cells.

Gene	Microarray (Fold change ± SD)				qRT-PCR (Fold change)			
	1 h	3 h	6 h	24 h	1 h	3 h	6 h	24 h
ERCC1	-1.09±0.28	-1.03±0.24	1.54±0.06[b]	-2.76±0.20[b]	1.05	1.02	1.07	-1.27
ERCC2	1.08±0.11	-1.26±0.16	1.06±0.20	-3.79±0.11[c]	1.11	-1.14	-1.23	-1.39
MGMT	1.05±0.49	1.89±0.29	1.14±0.49	-2.60±0.31[a]	-1.02	-1.12	-1.20	-2.63
OGG1	1.09±0.56	-1.10±0.28	-1.48±0.63	-2.53±0.23[b]	1.13	-1.16	-1.27	-1.56
TP53	1.04±0.09	1.24±0.19	1.02±0.13	-1.50±0.08[a]	1.05	-1.45	-1.85	-1.15

SD, standard deviation. [a]P<0.05, [b]P<0.01, [c]P<0.001 as compared to control cells, n=3 for microarray and qRT-PCR analysis.
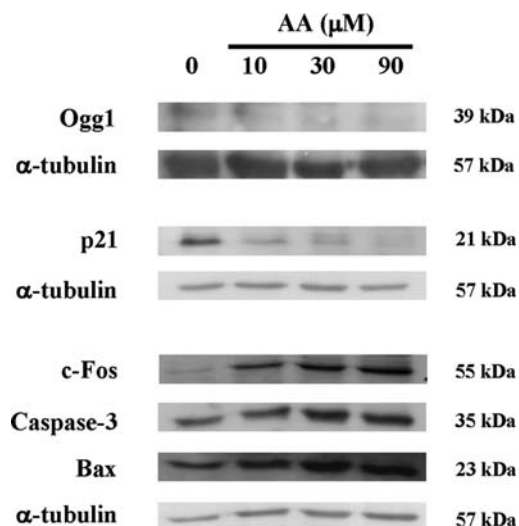

Figure 4. Effect of AA on the expression of DNA repair, cell cycle, apoptosis-related proteins. HK-2 cells were treated with 10, 30, 90 μM of AA for 24 h. Protein samples (45 μg each) were resolved by SDS-poly-acrylamide gel electrophoresis and transferred to nitrocellulose membranes. After blocking, the membranes were incubated overnight with antibodies specific to Ogg1, p21, c-fos, caspase-3, Bax and α-tubulin. They were then blotted with a secondary antibody conjugated with horseradish peroxidase, followed by detection using ECL substrate. α-tubulin was used as loading control.
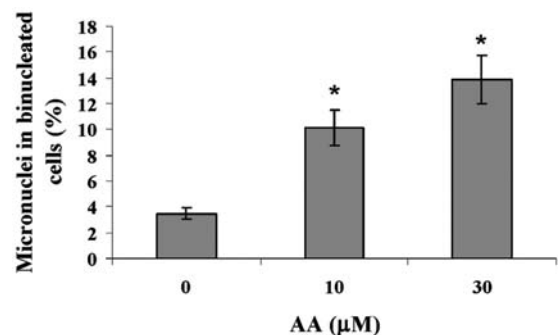
Figure 5. Induction of micronuclei formation by AA in HK-2 cells. HK-2 cells were treated with 10 and 30 μM of AA. Following treatment, the medium was replaced with fresh medium containing cytochalasin B (3 μg/ml) to obtain binucleated cells. Cells were cultured for at least 16 h prior to fixation and staining with acridine orange solution (0.1 mg/ml). The extent of chromosome damage was examined by scoring micronuclei formation in 1000 binucleated cells. *P<0.05, n=3.

Discussion

In the present study, we used toxicogenomic analysis to clarify the molecular mechanisms of AA-induced toxic effects in normal human proximal tubular cells. Among the genes that

were regulated by AA, we found that genes in DNA repair pathway were the most significantly altered after exposure to 10, 30 and 90 μM of AA. Furthermore, some genes related to stress response, cell cycle, apoptosis, fibrogenic response, and biotransformation were also significantly regulated by all AA treatments in HK-2 cells (Table III). Furthermore, the results from qRT-PCR analysis of the 8 selected genes (ERCC1, ERCC2, GADD45B, MGMT, NAIP, OGG1, PARP1, TP53) confirmed the results from the microarray analysis (Tables V and VI). AA significantly inhibited the mRNA expression of DNA repair-associated genes, including ERCC1, ERCC2, MGMT, OGG1, and PARP1. After AA treatment, the down-regulation of the gene and protein expression of OGG1, a specific DNA glycosylase that excises 8-OHdG, may partly explain the observed increased number of 8-OHdG-stained cells and increased levels of single strand breaks in AA-treated cells. Subsequently, the induction of DNA damage and the repression of DNA repair gene expression by AA resulted in a dose-dependent increase in the frequency of micronuclei formation in binucleated HK-2 cells (Fig. 5). Our results show the involvement of oxidative damage on AA-induced cytotoxicity and provide new insight into the possible involvement of DNA repair inhibition on AA-induced genotoxicity.

Herbal drugs derived from *Aristolochia* spp. have been known since antiquity and the anti-inflammatory properties of AA encouraged the development of pharmaceutical preparations in Germany until Mengs and co-workers observed that AA is a strong carcinogen in rats in 1982. Several studies showed that AA can induce cytotoxic effects in human colon cancer HCT 116 cells, porcine renal LLC-PK1 cells, and opossum kidney (OK) cell line. The HK-2 cells used in our study were more sensitive to the cytotoxicity of AA than HCT 116 cells (35), and OK cells (40). The IC$_{50}$ of 24 h AA treatment for HK-2 cells and HCT 116 cells was 30 and 100 μM, respectively. Incubation of OK cells with AA (10 or 20 μM) for 24 h was shown not to affect cell viability. The findings from those studies point out the importance of using cultured cells derived from normal human target organs of a specific chemical when its toxic effects to human are examined.

Our toxicogenomic analysis revealed that genes in biological processes of DNA repair, response to DNA damage stimuli, apoptosis, extracellular matrix organization and biogenesis, DNA-dependent DNA replication, and regulation of cell cycle were significantly regulated by AA in HK-2 cells. Among those processes, however, genes in the DNA repair pathway were the most significantly regulated (Table II). Among stress response-related genes, GADD45B (growth arrest and DNA-damage-inducible, ß gene) was significantly up-regulated by AA at all three of the tested concentrations (Table III). GADD45B, a member of a family of structurally related proteins including GADD45A and GADD45G, has been implicated in stress signaling in response to physiological and genotoxic stressors (41), which results in either cell cycle arrest, DNA repair, cell survival or apoptosis. On the other hand, aberrant expression of GADD45 has also been implicated in the development of cancer (42). Our finding that GADD45B was up-regulated by AA is consisted with that reported previously (43), in which GADD45B was

induced by the alkylating agent MMS (methylmethane sulfonate) and sorbitol.

Previous studies in LLC-PK1 cells showed that AAI induced apoptotic damage by inhibiting the increase of intracellular free calcium concentration. Our study from microarray analysis revealed the increase expression of the pro-apoptotic factors, BAX and caspase, after AA exposure. BAX (BCL2-associated X protein gene) was up-regulated at high dose (90 μM) in HK-2 cells (Table III). Caspase-3 was up-regulated at 30 μM AA treatment and these results are similar to reports from Balachandran *et al* (31). They found that the caspase activity was induced by AAI, AAII, AAIa, and AAVIIIa in LLC-PK1 cells. Our Western blot analysis showed AA induced a dose-dependent increase of BAX and caspase-3 protein. NAIP (apoptosis inhibitor protein) is overexpressed in most human cancers and inhibition of its function results in increased apoptosis. The role of up-regulation of NAIP in AA-induced cytotoxicity needs further investigation.

Among cell cycle-related genes, the gene and protein expression levels of CDKN1A (cyclin-dependent kinase inhibitor 1A, p21) were down-regulated after 10 μM AA treatment. CDKN1A mediates the p53-dependent cell cycle G1 phase arrest in response to a variety of stress signals, including genotoxic stress, hypoxia, and oncogene activation. Our results were opposite to those reported (35) in p53-null cells after a 48-h exposure to AA (100 μM) in HCT 116 cell line. Previous data from Chang (33) showed that AA mixture (AAM; 41% AA I, 56% AA II) can cause arrest in the G0/G1 phase (from 37.6 to 49.2%) in human urinary tract epithelium cells (SV-HUC-1), suggesting that AA-induced cell cycle arrest at the G0/G1 phase is associated with cyclin E/cdk2 complex (the cdk inhibitor). They also found that the levels of cell cycle control protein (include p53, p21 and p27) were increased in a concentration-dependent manner after AA exposure for 24 h. Our Western blot analysis found that p21 protein expression was dramatically decreased after exposure to all three doses of AA.

MDM2, another gene involved in the cell cycle, is a target gene of the transcription factor p53. Our observation that MDM2 is significantly down-regulated by AA is similar to that reported in AA-treated wild-type rats (44). Overexpression of MDM2 can result in excessive inactivation of p53, thereby diminishing its tumor suppressor function. The tumor suppressor p53 also affects the cell cycle, apoptosis, and tumorigenesis through interactions with other proteins. p53 is activated in response to DNA damage due to ultraviolet light, chemicals, or ionizing radiation. It is generally believed that the activity of p53 is primarily governed by its protein level. The immediate early gene c-fos is a cellular proto-oncogene that belongs to the fos family of transcription factors. The c-fos protein codes for a major nuclear target that dimerizes with c-Jun to form AP-1 transcription factor complexes, which in turn participate in many cellular events including cell proliferation, differentiation, apoptosis, and stress responses. Fos was significantly up-regulated by AA treatment (90 μM) in HK-2 cells in our study but was shown to be significantly down-regulated in HCT 116 cancer cell line (35).

AA was shown to causes chromosomal aberration in human lymphocytes *in vitro* and increases the mutation

frequency of *lacZ* and *CII* locus in *lambda/lacZ* transgenic mice *in vivo*. Cosyns *et al* have found that urothelial carcinomas are associated with overexpression of p53 protein in AAN patients (45). Lord *et al* (46) detected a specific AAG-to-TAG mutation in codon 139 of exon 5 in TP53 in DNA from one patient with AAN-associated urothelial carcinoma. That mutation in the TP53 gene might trigger tumorigenesis in AAN patients in the same way that AA-induced mutations in codon 61 of H-ras trigger tumorigenesis in rodents (47). In our study, microarray expression profile and quantification by RT-PCR showed that 10, 30 and 90 μM treatment of AA could down-regulate *TP53*. These results differ from those reported by Simoes *et al* (35) in which no significant difference in p53 expression was found in p53-WT HCT 116 cells after a 24-h exposure to AA (100 μM). Many studies have showed that *TP53* is involved in the nucleotide excision repair pathway and that loss of *TP53* will enhance DNA damage (48-50). Shen *et al* (50) showed that arsenic can cause genotoxicity by inhibiting the p53-medicated nucleotide excision repair. Tsai *et al* (49) showed that arecoline, which is a major alkaloid of areca nut, can repress p53-activated DNA repair and induce DNA damage in human epithelial cells. Our microarray and qRT-PCR data showed that AA caused the down-regulation of TP53 which may lead to the decrease of DNA repair capability and subsequently induce tumorigenesis. Further study is needed to clarify the changes of p53 gene and protein expression after AA treatment.

Table IV shows the selected DNA repair genes that were significantly regulated by AA in HK-2 cells. Among those genes, nucleotide excision repair (NER) genes are most likely involved in repairing AA-DNA adducts. This is because NER genes are known to play a key role in preventing toxicity and mutation frequencies for bulky, distortive DNA lesions. The NER process includes damage recognition, local opening of the DNA duplex around the lesion, dual incision of the damaged DNA strand, gap repair synthesis, and strand ligation (51). The NER pathway splits into two sub-pathways: transcription-coupled repair (TCR) and global genomic repair (GGR). They are fundamentally identical except in steps of damage recognition. In humans, NER is a major protector against the carcinogenic effect of UV light and inborn defects such as xeroderma pigmentosum (XP) (52). ERCC1 (excision repair cross-complementing group 1) and ERCC2 (XPD) (excision repair cross-complementing rodent repair deficiency, complementation group 2; xeroderma pigmentosum D) belong to NER-deficient complementation groups. The ERCC1 domain is a part of endonuclease (5's incision) during DNA strand dual incision step (53) and overexpression of ERCC1 mRNA is related to cisplatin resistance in gastric, ovarian and lung cancer (54-56). ERCC1 expression was also reported to be a specific target for oxidative stress-induced modification of NER (57). ERCC2 (XPD) is involved in both GGR and TCR and is an integral member of the basal transcription factor BTF2/TFIIH complex. Defects in this gene can result in three different disorders, the cancer-prone syndrome xeroderma pigmentosum complementation group D, trichothiodystrophy and Cockayne syndrome (58). Our study found that ERCC1 and ERCC2 were both down-regulated by AA. Similar findings were reported by Cheng *et al* (59) and Wei *et al* (60) they found that low mRNA

levels of DNA-repair genes (including ERCCC1 and ERCC2) in lymphocytes were associated with high relative risk for head and neck cancer and lung cancer. The decreased expression of ERCC1 by AA treatment is also in accordance to the study in which arsenic can diminish the expression of the nucleotide excision repair genes ERCC1, XPF (ERCC4), and XPB (ERCC3) (61). Another DNA repair gene, MGMT (O-6-methylguanine-DNA methyltransferase), was down-regulated in 30 μM AA treatment but this result is opposite to that in AA-treated rats (44).

It is well known that reactive oxygen species (ROS) can cause oxidative damage to DNA. Our transcriptome analysis revealed that AA exposure caused a down-regulation of the gene expression of antioxidant enzymes, such as superoxide dismutase, glutathione reductase, and glutathione peroxidase. Furthermore, we found that AA induced an oxidative stress characterized by an induction of 8-OHdG and DNA strand breaks. These results suggest that the involvement of oxidative stress in AA-induced toxicity. 8-OHdG, one of the major abundant oxidative DNA damage markers which can efficiently repair by a glycosylase, OGG1 (62-65). In this study, gene expression of OGG1 was decreased in cells exposed to AA. Microarray analysis showed a 2.5-fold decrease and qRT-PCR showed a 1.6-fold decrease in OGG1 gene expression in cells exposed to AA. Furthermore, there was a dose-dependent increase in 8-OH-dG immunostaining, probably as a result of decreased OGG1 expression. We also used comet assay to examine DNA damage in HK-2 cells after exposure to AA. The results showed a significant increase in the tail movement at all concentrations (Fig. 2) (p<0.05). These findings were similar to those reported by Wu *et al* (34). They used comet and micronucleus test to identify the genotoxicity of AA and found a clear dose-dependent manner (25-200 μM AA) increase in tail DNA movement and a significant increase in frequencies of micronuclei (12.5-50 μM AA) in human hepatoma HepG2 cells (34). They also found that AA at concentrations $\geq$50 μM caused a significant increase in NO and 8-OHdG levels and assumed that high-dose AA exerted genotoxicity probably via NO in HepG2 cells. It is worthwhile to note that the expression and activity of hOGG1 is thought to be primarily regulated by p53 (66). In our study, OGG1 and TP53 were both significantly down-regulated in cells exposed to AA.

In conclusion, in this study, we applied toxicogenomic analysis to explore the changes in gene expression after AA exposure. The genes that were most significantly regulated by AA treatment at doses of 10, 30 and 90 μM involved in DNA repair, cell cycle, apoptosis, and response to DNA damage. All treatments with AA effectively down-regulated genes involved in DNA repair. The inhibition of DNA repair gene expression by AA was further confirmed by qRT-PCR. Moreover, comet assay, immunostaining, and micronucleus assay showed that AA caused oxidative DNA damage and chromosome damage. The down-regulation of OGG1 and other DNA repair genes by AA may subsequently have led to the observed increase in 8-OHdG and micronuclei in HK-2 cells, thereby leading to increased DNA damage. Our results provide new insight into the involvement of down-regulation of DNA repair gene expression as a possible mechanism for AA-induced mutagenesis and carcinogenesis.

References

1. Rosenmund H and Reichstein T: Zur Kenntnis der Aristolochiasäure. Pharm Acta Helv 18: 243-261, 1943.
2. Zhang G, Shimokawa S, Mochizuki M, Kumamoto T, Nakanishi W, Watanabe T, Ishikawa T, Matsumoto K, Tashima K, Horie S, Higuchi Y and Dominguez OP: Chemical constituents of Aristolochia constricta: antispasmodic effects of its constituents in guinea-pig ileum and isolation of a diterpeno-lignan hybrid. J Nat Prod 71: 1167-1172, 2008.
3. Messiano GB, Vieira L, Machado MB, Lopes LM, de Bortoli SA and Zukerman-Schpector J: Evaluation of insecticidal activity of diterpenes and lignans from Aristolochia malmeana against Anticarsia gemmatalis. J Agric Food Chem 56: 2655-2659, 2008.
4. Debelle FD, Vanherweghem JL and Nortier JL: Aristolochic acid nephropathy: a worldwide problem. Kidney Int 74: 158-169, 2008.
5. Mengs U, Lang W and Poch J-A: The carcinogenic action of aristolochic acid in rats. Arch Toxicol 51: 107-119, 1982.
6. Vanherweghem JL, Depierreux M, Tielemans C, *et al*: Rapidly progressive interstitial renal fibrosis in young women: association with slimming regimen including Chinese herbs. Lancet 341: 387-391, 1993.
7. Vanhaelen M, Vanhaelen-Fastre R, But P and Vanherweghem JL: Identification of aristolochic acid in Chinese herbs. Lancet 343: 174, 1994.
8. Stengel B and Jones E: [End-stage renal insufficiency associated with Chinese herbal consumption in France]. Nephrologie 19: 15-20, 1998.
9. Lord GM, Tagore R, Cook T, *et al*: Nephropathy caused by Chinese herbs in the UK. Lancet 354: 481-482, 1999.
10. Arlt VM, Stilborova M and Schmeiser HH: Aristolochic acid as a probable human cancer hazard in herbal remedies: a review. Mutagenesis 17: 265-277, 2002.
11. Cosyns JP, Jadou lM, Squifflet JP, *et al*: Chinese herbs nephropathy: a clue to Balkan endemic nephropathy? Kidney Int 45: 1680-1688, 1994.
12. Depierreux M, Damme BV, Vanden HK, *et al*: Pathologic aspects of a newly described nephropathy related to the prolonged use of Chinese herbs. Am J Kidney Dis 24: 172-180, 1994.
13. Nortier JL, Martinez MC, Schmeiser HH, Arlt VM, Bieler CA, Petein M, Depierreux MF, De Pauw L, Abramowicz D, Vereerstraeten P and Vanherweghem JL: Urothelial carcinoma associated with the use of a Chinese herb (Aristolochia fangchi). N Engl J Med 342: 1686-1692, 2000.
14. Cosyns JP, Jadoul M, Squifflet JP, Van Cangh PJ and van Ypersele de Strihou C: Urothelial malignancy in nephropathy due to Chinese herbs. Lancet 344: 188, 1994.
15. Lai MN, Wang SM, Chen PC, Chen YY and Wang JD: Population-based case-control study of Chinese herbal products containing aristolochic acid and urinary tract risk. J Natl Cancer Inst 102: 1-8, 2009.
16. Lai MN, Lai JN, Chen PC, Hsieh SC, Hu FC and Wang JD: Risks of kidney failure associated with consumption of herbal products containing Mu Tong or Fangchi: a population based case-control study. Am J Kidney Dis (In press).
17. Martinez MC, Nortier J, Vereestraeten P and Vanherweghem JL: progression rate of Chinese herb nephropathy: impact of Aristolochia fangchi ingested dose. Nephrol Dial Transplant 17: 408-412, 2002.
18. Schmeiser HH, Bieler CA, Wiessler M, van YdSC and Cosyns JP: Detection of DNA adducts formed by aristolochic acid in renal tissue from patients with Chinese herbs nephropathy. Cancer Res 56: 2025-2028, 1996.
19. Bieler CA, Stiborova M, Wiessler M, Cosyns JP, van Ypersele de Strihou C and Schmeiser HH: ^{32}P-post-labelling analysis of DNA adducts formed by aristolochic acid in tissues from patients with Chinese herbs nephropathy. Carcinogenesis 18: 1063-1067, 1997.
20. Schmeiser HH, Schoepe KB and Wiessler M: DNA adduct formation of aristolochic acid I and II in vitro and in vivo. Carcinogenesis 9: 297-303, 1988.
21. Stiborova M, Fernando RC, Schmeiser HH, Frei E, Pfau W and Wiessler M: Characterization of DNA adducts formed by aristolochic acids in the target organ (forestomach) of rats by ^{32}P-postlabelling analysis using different chromatographic procedures. Carcinogenesis 15: 1187-1192, 1994.
22. Stiborova M, Bieler CA, Wiessler M and Frei E: The anti-cancer agent ellipticine on activation by cytochrome P450 forms covalent DNA adducts. Biochem Pharmacol 62: 1675-1684, 2001.
23. Stiborova M, Frei E, Breuer A, Wiessler M and Schmeiser HH: Evidence for reductive activation of carcinogenic aristolochic acids by prostaglandin H synthase - (32)P-postlabeling analysis of DNA adduct formation. Mutat Res 493: 149-160, 2001.
24. Stiborova M, Frei E, Wiessler M and Schmeiser HH: Human enzymes involved in the metabolic activation of carcinogenic aristolochic acids: evidence for reductive activation by cytochromes P450 1A1 and 1A2. Chem Res Toxicol 14: 1128-1137, 2001.
25. Stiborova M, Hajek M, Frei E and Schmeiser HH: Carcinogenic and nephrotoxic alkaloids aristolochic acids upon activation by NADPH: cytochrome P450 reductase form adducts found in DNA of patients with Chinese herbs nephropathy. Gen Physiol Biophys 20: 375-392, 2001.
26. Stiborova M, Schmeiser HH, Breuer A and Frei E: Evidence for activation of carcinogenic o-anisidine by prostaglandin H synthase: ^{32}P-postlabelling analysis of DNA adduct formation. Gen Physiol Biophys 20: 267-279, 2001.
27. Broschard TH, Wiessler M and Schmeiser HH: Effect of site-specifically located aristolochic acid DNA adduct on in vitro DNA synthesis by human DNA polymerase alpha. Cancer Lett 98: 47-56, 1995.
28. Arlt VM, Pfohl-Leszkowicz A, Cosyns J and Schmeiser HH: Analyses of DNA adducts formed by ochratoxin A and aristolochic acid in patients with Chinese herbs nephropathy. Mutat Res 494: 143-150, 2001.
29. Gillerot G, Jadoul M, Arlt VM, van Ypersele De Strihou C, Schmeiser HH, But PP, Bieler CA and Cosyns JP: Aristolochic acid nephropathy in a Chinese patient: time to abandon the term 'Chinese herbs nephropathy'? Am J Kidney Dis 38: E26, 2001.
30. Lord GM, Cook T, Arlt VM, Schmeiser HH, Williams G and Pusey CD: Urothelial malignant disease and Chinese herbal nephropathy. Lancet 358: 1515-1516, 2001.
31. Balachandran P, Wei F, Lin RC, Khan IA and Pasco DS: Structure activity relationships of aristolochic acid analogues: toxicity in cultured renal epithelial cells. Kidney Int 67: 1797-1805, 2005.
32. Li Y, Liu Z, Guo X, Shu J, Chen Z and Li L: Aristolochic acid I-induced DNA damage and cell cycle arrest in renal tubular epithelial cells in vitro. Arch Toxicol 80: 524-532, 2006.
33. Chang HR, Lian JD, Lo CW, Huang HP and Wang CJ: Aristolochic acid-induced cell cycle G1 arrest in human urothelium SV-HUC-1 cells. Food Chem Toxicol 45: 396-402, 2007.
34. Wu K, Jiang L, Cao J, Yang G, Geng C and Zhong L: Genotoxic effect and nitrative DNA damage in HepG2 cells exposed to aristolochic acid. Mutat Res 630: 97-102, 2007.
35. Simoes ML, Hockley SL, Schwerdtle T, Gamboa da Costa G, Schmeiser HH, Phillips DH and Arlt VM: Gene expression profiles modulated by the human carcinogen aristolochic acid I in human cancer cells and their dependence on TP53. Toxicol Appl Pharmacol 232: 86-98, 2008.
36. Chen T, Guo L, Zhang L, Shi L, Fang H, Sun Y, Fuscoe JC and Mei N: Gene expression profiles distinguish the carcinogenic effects of aristolochic acid in target (Kidney) and non-target (liver) tissues in rats. BMC Bioinformatics 7 (Suppl. 2): S20, 2006.
37. Cheng WY, Hsiang CY, Bau DT, Chen JC, Shen WS, Li CC, Lo HY, Wu SL, Chiang SY and Ho TY: Microarray analysis of vanillin-regulated gene expression profile in human hepato-carcinoma cells. Pharmacol Res 56: 474-482, 2007.

38. Smyth GK: Limma: linear models for microarray data. In: Bioinformatics and computational biology solutions using R and bioconductor. Gentleman R, Carey V, Dudoit S, Irizarry R and Huber W (eds). New York, pp397-420, 2005.
39. Montaner D, Tarraga J, Huerta-Cepas J, Burguet J, Vaquerizas JM, Conde L, Minguez P, Vera J, Mukherjee S, Valls J, Pujana MA, Alloza E, Herrero J, Al-Shahrour F and Dopazo J: Next station in microarray data analysis: GEPAS. Nucleic Acids Res 34: W486-W491, 2006.
40. Lebeau C, Arlt VM, Schmeiser HH, Boom A, Verroust PJ, Devuyst O and Beauwens R: Aristolochic acid impedes endocytosis and induces DNA adducts in proximal tubule cells. Kidney Int 60: 1332-1342, 2001.
41. Liebermann DA and Hoffman B: Gadd45 in stress signaling. J Mol Signal 3: 15, 2008.
42. Cretu A, Sha X, Tront J, Hoffman B and Liebermann DA: Stress sensor Gadd45 genes as therapeutic targets in cancer. Cancer Ther 7: 268-276, 2009.
43. Zumbrun SD, Hoffman B and Liebermann DA: Distinct mechanisms are utilized to induce stress sensor gadd45b by different stress stimuli. J Cell Biochem 108: 1220-1231, 2009.
44. Stemmer K, Ellinger-Ziegelbauer H, Ahr HJ and Dietrich DR: Carcinogen-specific gene expression profiles in short-term treated Eker and wild-type rats indicative of pathways involved in renal tumorigenesis. Cancer Res 67: 4052-4068, 2007.
45. Cosyns JP, Jadoul M, Squifflet JP, Wese FX and van Ypersele de Strihou C: Urothelial lesions in Chinese-herb nephropathy. Am J Kidney Dis 33: 1011-1017, 1999.
46. Lord GM, Hollstein M, Arlt VM, Roufosse C, Pusey CD, Cook T and Schmeiser HH: DNA adducts and p53 mutations in a patient with aristolochic acid-associated nephropathy. Am J Kidney Dis 43: e11-17, 2004.
47. Schmeiser HH, Scherf HR and Wiessler M: Activating mutations at codon 61 of the c-Ha-ras gene in thin-tissue sections of tumors induced by aristolochic acid in rats and mice. Cancer Lett 59: 139-143, 1991.
48. Lloyd DR and Hanawalt PC: p53-dependent global genomic repair of benzo[a]pyrene-7,8-diol-9,10-epoxide adducts in human cells. Cancer Res 60: 517-521, 2000.
49. Tsai YS, Lee KW, Huang JL, Liu YS, Juo SH, Kuo WR, Chang JG, Lin CS and Jong YJ: Arecoline, a major alkaloid of areca nut, inhibits p53, represses DNA repair, and triggers DNA damage response in human epithelial cells. Toxicology 249: 230-237, 2008.
50. Shen S, Lee J, Weinfeld M and Le XC: Attenuation of DNA damage-induced p53 expression by arsenic: a possible mechanism for arsenic co-carcinogenesis. Mol Carcinog 47: 508-518, 2008.
51. Wood RD: Nucleotide excision repair in mammalian cells. J Biol Chem 272: 23465-23468, 1997.
52. Conforti G, Nardo T, D'Incalci M and Stefanini M: Proneness to UV-induced apoptosis in human fibroblasts defective in transcription coupled repair is associated with the lack of Mdm2 transactivation. Oncogene 19: 2714-2720, 2000.
53. Wood RD, Araujo SJ, Ariza RR, Batty DP, Biggerstaff M, Evans E, Gaillard PH, Gunz D, Koberle B, Kuraoka I, Moggs JG, Sandall JK and Shivji MK: DNA damage recognition and nucleotide excision repair in mammalian cells. Cold Spring Harb Symp Quant Biol 65: 173-182, 2000.
54. Metzger R, Leichman CG, Danenberg KD, Danenberg PV, Lenz HJ, Hayashi K, Groshen S, Salonga D, Cohen H, Laine L, Crookes P, Silberman H, Baranda J, Konda B and Leichman L: ERCC1 mRNA levels complement thymidylate synthase mRNA levels in predicting response and survival for gastric cancer patients receiving combination cisplatin and fluorouracil chemotherapy. J Clin Oncol 16: 309-316, 1998.
55. Dabholkar M, Vionnet J, Bostick-Bruton F, Yu JJ and Reed E: Messenger RNA levels of XPAC and ERCC1 in ovarian cancer tissue correlate with response to platinum-based chemotherapy. J Clin Invest 94: 703-708, 1994.
56. Lord RV, Brabender J, Gandara D, Alberola V, Camps C, Domine M, Cardenal F, Sanchez JM, Gumerlock PH, Taron M, Sanchez JJ, Danenberg KD, Danenberg PV and Rosell R: Low ERCC1 expression correlates with prolonged survival after cisplatin plus gemcitabine chemotherapy in non-small cell lung cancer. Clin Cancer Res 8: 2286-2291, 2002.
57. Langie SA, Knaapen AM, Houben JM, van Kempen FC, de Hoon JP, Gottschalk RW, Godschalk RW and van Schooten FJ: The role of glutathione in the regulation of nucleotide excision repair during oxidative stress. Toxicol Lett 168: 302-309, 2007.
58. Caggana M, Kilgallen J, Conroy JM, Wiencke JK, Kelsey KT, Miike R, Chen P and Wrensch MR: Associations between ERCC2 polymorphisms and gliomas. Cancer Epidemiol Biomarkers Prev 10: 355-360, 2001.
59. Cheng L, Sturgis EM, Eicher SA, Spitz MR and Wei Q: Expression of nucleotide excision repair genes and the risk for squamous cell carcinoma of the head and neck. Cancer 94: 393-397, 2002.
60. Wei Q, Wang LE, Sturgis EM and Mao L: Expression of nucleotide excision repair proteins in lymphocytes as a marker of susceptibility to squamous cell carcinomas of the head and neck. Cancer Epidemiol Biomarkers Prev 14: 1961-1966, 2005.
61. Andrew AS, Karagas MR and Hamilton JW: Decreased DNA repair gene expression among individuals exposed to arsenic in United States drinking water. Int J Cancer 104: 263-268, 2003.
62. Mei N, Kunugita N, Hirano T and Kasai H: Acute arsenite-induced 8-hydroxyguanine is associated with inhibition of repair activity in cultured human cells. Biochem Biophys Res Commun 297: 924-930, 2002.
63. Kinoshita A, Wanibuchi H, Wei M, Yunoki T and Fukushima S: Elevation of 8-hydroxydeoxyguanosine and cell proliferation via generation of oxidative stress by organic arsenicals contributes to their carcinogenicity in the rat liver and bladder. Toxicol Appl Pharmacol 221: 295-305, 2007.
64. Ma H, Wang J, Abdel-Rahman SZ, Boor PJ and Khan MF: Oxidative DNA damage and its repair in rat spleen following subchronic exposure to aniline. Toxicol Appl Pharmacol 233: 247-253, 2008.
65. Kang KA, Lee JH, Chae S, Zhang R, Piao MJ, Kim HS, You HJ and Hyun JW: Butin decreases oxidative stress-induced 8-hydroxy-2'-deoxyguanosine levels via activation of oxoguanine glycosylase 1. Chem Biol Interact 181: 338-342, 2009.
66. Chatterjee A, Mambo E, Osada M, Upadhyay S and Sidransky D: The effect of p53-RNAi and p53 knockout on human 8-oxoguanine DNA glycosylase (hOgg1) activity. FASEB J 20: 112-114, 2006.